



POTSDAM-INSTITUT FÜR
KLIMAFOLGENFORSCHUNG

Originally published as:

[Maskell, G. M.](#), [Chemura, A.](#), Nguyen, H., [Gornott, C.](#), Mondal, P. (2021): Integration of Sentinel optical and radar data for mapping smallholder coffee production systems in Vietnam. - Remote Sensing of Environment, 266, 112709.

DOI: <https://doi.org/10.1016/j.rse.2021.112709>

1 Integration of Sentinel optical and radar data for mapping smallholder coffee
2 production systems in Vietnam

3 Authors

4 Gina Maskell^{a,b,*}, Abel Chemura^a, Huong Nguyen^c, Christoph Gornott^{a,d,°}, Pinki Mondal^{e,f,°}

5 a Potsdam Institute for Climate Impact Research (PIK), Potsdam, Germany

6 b Albrecht Daniel Thaer Institute for Agricultural and Horticultural Sciences, Humboldt University Berlin, Berlin, Germany

7 c Department of Forest Resource & Environment Management (FREM), Tay Nguyen University, Dak Lak Province, Vietnam

8 d Department of Agroecosystem Analysis and Modelling, University of Kassel, Kassel, Germany

9 e Department of Geography and Spatial Sciences, University of Delaware, Newark, DE, United States of America

10 f Department of Plant and Soil Sciences, University of Delaware, Newark, DE, United States of America

11 * corresponding author, maskell@pik-potsdam.de

12 ° shared last authorship

13

14 Abstract

15 Perennial commodity crops, such as coffee, often play a large role globally in agricultural
16 markets and supply chains and locally in livelihoods, poverty reduction, and biodiversity. Yet,
17 the production of spatial information on these crops are often overlooked in favor of annual
18 food crops. Remote sensing detection of coffee faces a particular set of challenges due to
19 persistent cloud cover in the tropical “coffee belt,” hilly topography in coffee growing regions,
20 diversity of coffee growing systems, and spectral similarity to other tree crops and agricultural
21 land. Looking at the major coffee growing region in Dak Lak, Vietnam, we integrate multi-
22 temporal 10m optical Sentinel-2 and Sentinel-1 SAR data in order to map three coffee
23 production systems: i) open-canopy sun coffee, ii) intercropped and other shaded coffee and
24 iii) newly planted or young coffee.

25

26 Leveraging Google Earth Engine (GEE), we compute five sets of features in order to best
27 enhance separability *between* coffee and other land cover *and within* coffee production
28 systems. The features include Sentinel-2 dry and wet season composites, Sentinel-1 texture
29 features, Sentinel-1 spatiotemporal metrics, and topographic features. Using a random forest

30 classification algorithm, we produce a 9-class land cover map including our three coffee
31 production classes and a binary coffee / non-coffee map. The binary map has an overall
32 accuracy of 89% and the three coffee production systems have user accuracies of 65, 56,
33 71% for sun coffee, intercropped coffee and newly planted coffee, respectively. This is a first
34 effort at large-scale distinction of within-crop production styles and has implications across
35 many applications. The binary coffee map can be used as a high-resolution crop mask,
36 whereas the detailed land cover map can inform monitoring of deforestation dynamics,
37 biodiversity, sustainability certification and implementation of climate adaptation strategies.
38 This work offers a scalable approach to integrating optical and radar Sentinel data for
39 production of spatially explicit agricultural information and contributes particularly to tree crop
40 and agroforestry mapping, which often is overlooked in between agricultural and forestry
41 sciences.

42

43 Key words: agroforestry, smallholder agriculture, crop mask, Sentinel-1, Sentinel-2, data
44 fusion, Google Earth Engine, random forest

45

46 1. Introduction

47 Tree crops contribute to food and livelihood security, poverty alleviation, agricultural Gross
48 Domestic Product (GDP) and export earnings of tropical countries, especially commodity
49 crops such as coffee, cocoa and rubber (Dawson et al., 2014; Ha and Shively, 2007;
50 Läderach et al., 2017; Leakey, 2017). Over 70 tropical countries contribute to global coffee
51 production, now over 10 million tons annually (FAO, accessed: 01-11-2020). In Vietnam, the
52 2nd largest coffee producer worldwide, production is dominated by smallholders owning less
53 than 2 ha farmland (Fridell, 2014). There is an increasing demand for detailed information on
54 the spatial dynamics of such commodity tree crops to better understand deforestation
55 drivers, sustainability certification, livelihood preservation, and how a changing climate
56 intersects with these aspects (Hunt et al., 2020; Pham et al., 2019). However, accurately
57 mapping coffee production systems, especially distinguishing shade or intercropped system

58 (e.g. multi-canopy) and young coffee, remains challenging. Our study contributes to this
59 effort by building on applied remote sensing methods to derive cropped areas and planting
60 styles in the coffee landscape in Dak Lak province, Vietnam. In this study, we focus on the
61 robusta (*Coffea robusta*) growing region in Dak Lak, as there is a significantly less research
62 on robusta compared to arabica (*Coffea arabica*), worldwide (Hunt et al., 2020; Kath et al.,
63 2020; Pham et al., 2019).

64
65 Coffee in Vietnam is grown in a variety of agroecosystems. After many years of mostly sun-
66 grown coffee production systems with regional implications for reduced habitat, biodiversity
67 and water-resource related ecosystem services, Vietnam smallholders have recently shown
68 interest in diversification and more sustainable production, due to various economic and
69 climatic factors (Pham et al., 2020; Thi and Chaovanapoonphol, 2014). This diversification
70 has resulted in mixed agroforestry systems, such as intercropped plots where e.g.
71 peppercorn, fruit and nut trees are grown in between coffee trees, or nitrogen-fixing boundary
72 trees are planted on plot borders. In Vietnam, the focus is on “intercropping” systems, similar
73 to terms like shade, polyculture, multi-layer canopy. These production systems all entail that
74 multiple tree species are planted alongside coffee. These coffee production systems all have
75 their ecosystem service benefits in micro-climate temperature regulation, water retention
76 (through reduced evapotranspiration), increase in biodiversity and even coffee quality (De
77 Beenhouwer et al., 2013; de Carvalho et al., 2020; Jezeer et al., 2019; Nesper et al., 2017).
78 We are therefore motivated to not only map coffee area but to also separate coffee sub-
79 classes, including a distinction between sun and intercropped coffee as a means of
80 investigating on-the-farm agroforestry implementation.

81

82 1.1. Current Literature

83 Accurately mapping smallholder coffee production systems, especially the intercropped
84 coffee plots, has been challenging despite recent advances in remote sensing data and
85 methods. This challenge is compounded in that coffee and particularly intercropped systems

86 are often associated with complex and diverse management practices, which influences
87 spectral signal in various ways (Hung Anh et al., 2019; Nogueira et al., 2018). There is
88 limited work on distinguishing coffee production systems, i.e. coffee sub-categories (Hunt et
89 al., 2020). Only a handful of studies have distinguished shade (closed-canopy or mixed)
90 coffee from sun coffee (open-canopy or production) at mid-resolutions, such as Landsat
91 (Cordero-Sancho and Sader, 2007; Kawakubo and Pérez Machado, 2016; Ortega-Huerta et
92 al., 2012). Even fewer works distinguish coffee age classes (Chemura et al., 2017; Chemura
93 and Mutanga, 2016). And a single work classifies multiple production systems: closed
94 canopy, shade polyculture, sun monoculture and newly planted (sparse cover), using high
95 resolution IKONOS imagery (Widayati et al., 2003).

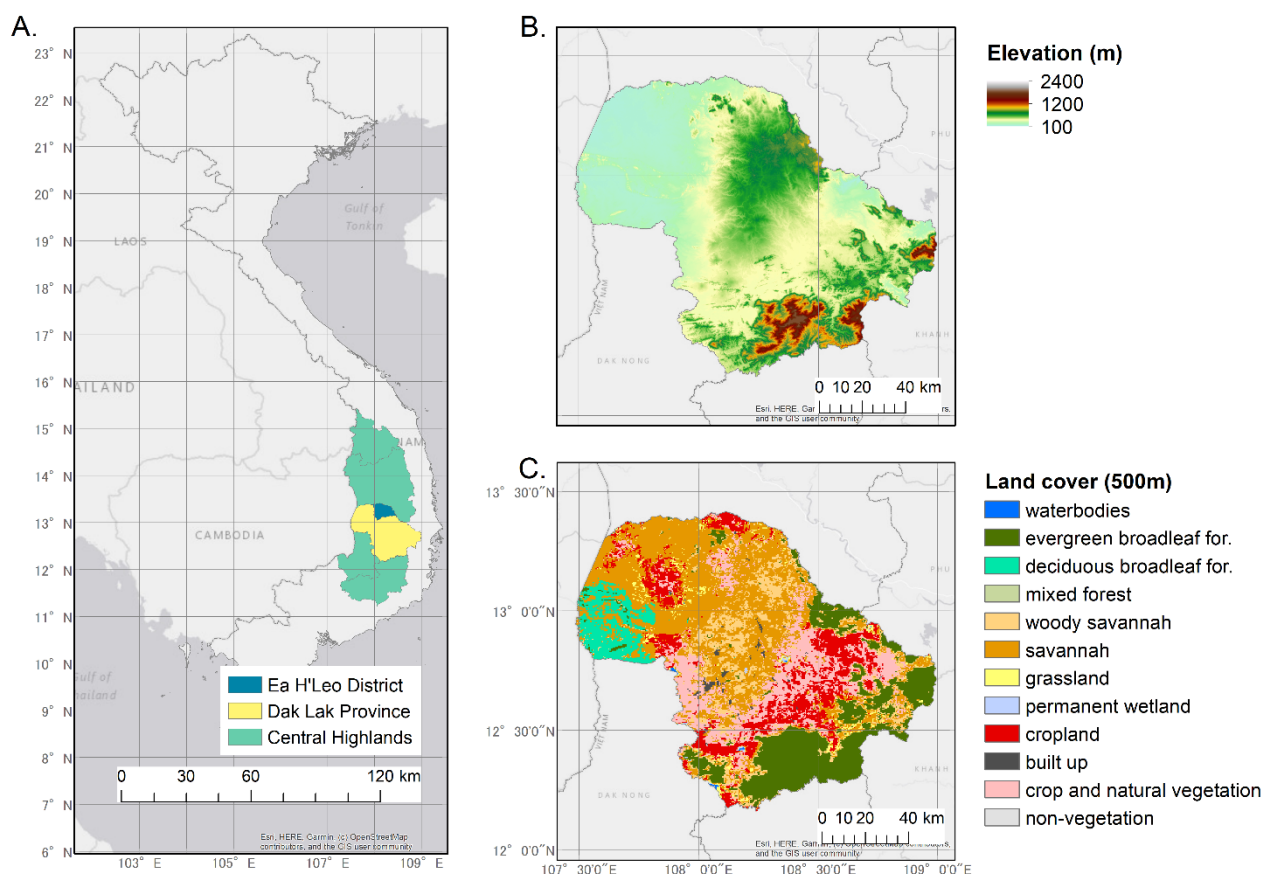
96

97 There are many documented challenges to mapping in coffee landscapes using remotely
98 sensed imagery, namely: (i) diversity in size and structure of coffee fields, (ii) steep slopes
99 and their topographic effects, (iii) wet season cloud coverage in coffee-growing tropics, and
100 (iv) similarity in the infrared spectral signal of coffee farms and adjacent mature plantations,
101 young plantations and agricultural land (Cordero-Sancho and Sader, 2007; Gomez et al.,
102 2010; Kelley et al., 2018; Mukashema et al., 2014; Nogueira et al., 2018; Ortega-Huerta et
103 al., 2012). The fusion of optical and synthetic aperture radar (SAR, specifically Sentinel-1
104 and Sentinel-2 data) has been highlighted as particularly promising for coffee mapping (Hunt
105 et al., 2020). Inclusion of Sentinel-1 has the main advantage that it is not restricted by cloud
106 coverage, a common barrier during the tropical rainy season. There are a growing number of
107 studies integrating these two data types in plantation mapping (Liu and Chen, 2019;
108 Poortinga et al., 2019), annual crop mapping (Clerici et al., 2017; Denize et al., 2018; Jin et
109 al., 2019; Mercier et al., 2019; Qadir and Mondal, 2020; Sun et al., 2019) and even detection
110 of single trees outside of forests (Brandt and Stolle, 2021); however, the integration of
111 Sentinel-1 and 2 data has not yet been applied to coffee production systems.

112

113 Along the same line of fusion of multiple satellite data, the integration of multiple remote
114 sensing derived feature types (e.g. not only spectral, but including texture, weather
115 indicators, topographic) has also been shown to be beneficial in heterogenous agricultural
116 and coffee mapping (Gomez et al., 2010; Hunt et al., 2020; Kelley et al., 2018). Most
117 commonly, topographic information is regularly included in many coffee mapping studies
118 (Cordero t Sancho and Sa
119 al., 2014), which can be attributed to coffee's suitability at higher elevations (DaMatta et al.,
120 2007). Precipitation or temperature features (Cordero d Sancho, 2007; Kelley et
121 al., 2018) and texture features (Gaertner, 2017; Gomez et al., 2010; Tsai and Chen, 2017)
122 are rapidly becoming key in difficult-to-map coffee regions. Studies that include texture
123 features often use high-resolution proprietary data such as WorldView (Gaertner, 2017) or
124 Quickbird (Gomez et al., 2010), or focus on mapping or distinguishing other tree crops such
125 as cocoa, rubber, oil palm (Burnett et al., 2019; Gao et al., 2015; Nomura and Mitchard,
126 2018; Numbisi et al., 2019; Torbick et al., 2016). Notably, Gray Level Co-occurrence
127 Matrices (GLCM) texture measures were derived from Sentinel-1 for cocoa mapping in
128 Numbisi et al. (2019). Texture measures were demonstrated to have more use in SAR
129 images compared to optical and are of added value in heterogenous landscapes (Mishra et
130 al., 2019).

131
132 We integrate Sentinel-2 optical and Sentinel-1 SAR data and generate the first map of its
133 kind for the different coffee production systems at the plot-level in Dak Lak, Vietnam. The
134 coffee production systems, or coffee subcategories that we target are: i) newly planted coffee
135 (< 3 years old), ii) intercropped coffee and iii) sun (open-canopy) coffee. We build on the
136 work of employing multiple feature types in a heterogenous smallholder landscape by
137 employing: optical spectral features, optical derived indices (such as vegetation indices),
138 SAR spectral and spatiotemporal features, SAR texture features, and topographic features.
139



140
 141 *Figure 1.* A) The Central Highlands region, Dak Lak province, and Ea H'Leo district; B)
 142 Elevation in Dak Lak (Farr et al., 2007) and C) Land cover map of Dak Lak, MODIS-derived
 143 land cover product (Friedl & Sulla-Menashe, 2015).

144
 145 **2. Study Area**

146 The province of Dak Lak (with an area of ~13,000 km²) is situated in the middle of the
 147 Central Highlands, a hilly region of Vietnam (Figure 1). The southern, high-elevation border is
 148 covered by tropical evergreen forest, and the northwestern, low-elevation corner by dry
 149 deciduous forest. A large portion of the province is dominated by agricultural land: perennials
 150 such as coffee, cashew, and rubber and annual crops such as rice and cassava. The Central
 151 Highlands has been defined as an “agricultural frontier region” (Agergaard et al., 2009;
 152 Grogan et al., 2015; Meyfroidt et al., 2013; Müller and Zeller, 2002; Phuc and Tran,
 153 2014). These frontier dynamics are often connected to cash crops, perennial crops grown for
 154 the external market such as a coffee and rubber (Meyfroidt et al., 2013). In the 1990s there
 155 was a “coffee boom,” where Vietnamese farmers planted over a million hectares (10,000

156 km²) of coffee (De Ha and Shively, 2007). More recently there is an emerging trend of forest
157 and annual cropland conversion for rubber plantations.

158

159 The coffee phenological cycle is many ways linked to seasonal weather patterns. The
160 Central Highlands has a dry season (December - March) and a wet (rainy) season (April -
161 November), with first rains in mid-April or early May and lasting into November (Pham -
162 Thanh et al., 2020). The flowering period for coffee occurs during the dry season, where
163 rainfall is low and evaporation is high. Because of this, farmers irrigate to start cherry
164 formation, primarily in January and February (Amarasinghe et al., 2015; Byrareddy, 2020;
165 Pham et al., 2020). The interactions between climate and management is a prominent
166 process occurring in the coffee landscape in Dak Lak and the Central Highlands.

167

168 3. Data and Methods

169 We combine optical and radar satellite data to create i) a detailed land cover map of the
170 coffee landscape (9 classes), targeting different coffee production classes and ii) a binary
171 map of coffee/non-coffee in order to characterize the spatial distribution of where coffee is
172 grown in Dak Lak. The model was developed on the basis of features and approaches from:
173 (a) Jin et al., (2019), who use multiple S1 & S2 features for crop mapping in a smallholder
174 landscape, (b) Poortinga et al., (2019), who integrate S1, S2, and Landsat-8 composites in a
175 tree crop landscape, and (c) Kelley et al., (2019), who map coffee using multiple data,
176 including optical seasonal composites, as well as through region-specific consideration in a
177 calibration phase. The more detailed land cover map can be used as a base map to examine
178 the evolution of different land uses/covers, whereas the binary map has applications as a
179 more traditional “crop mask.” To do this, we implement a random forest classifier in Google
180 Earth Engine (GEE) using optical, radar and topographic data as input features and training
181 and test data collected via Collect Earth relying on high-resolution imagery.

182

183 In order to best target such a complex target as coffee, we build our feature set and
184 approach based on the follow ecophysiological and plot characteristics of sun, intercropped
185 and new coffee:

186

187 *On separability of rubber and coffee:*

188 There are ecophysiological characteristics that can help distinguish mature rubber and sun
189 coffee. These are differences in foliage patterns, tree density and tree height. Coffee is an
190 evergreen tree while rubber is deciduous, losing leaves annually in the dry season. Rubber
191 trees are planted much closer together and almost quadruple the height of a mature coffee
192 tree (standing up to 20m tall and ~5m tall, respectively). We hypothesize that seasonal
193 optical imagery would capture the differences in foliage, particularly in the dry season, and
194 that S1 C-band backscatter would capture the double scatter of the coffee canopy and the
195 soil in a less dense sun coffee plot in order to distinguish these two dominant plantation
196 crops.

197

198 Additionally, coffee and rubber have different growing patterns, i.e. coffee is almost
199 exclusively planted in basaltic soils, often after clearing evergreen forests. Rubber, on the
200 other hand, is found in low-lying land, less constrained by soil type, and often organized in
201 expansive plots (very rarely in the same smallholder and ad-hoc patterns similar to coffee).
202 This spatial pattern can help to distinguish mature rubber and sun coffee, but also cleared
203 rubber from newly planted coffee. This hypothesis was demonstrated in part by the
204 importance of elevation in both the calibration of our classification model at the district level
205 in Ea H'Leo (Figure S1) and in our final land cover model at the province level of Dak Lak
206 (Figure S1 & S2).

207

208 Further, we also consider the timing of planting coffee saplings (at the beginning of the wet
209 season), for the distinction of newly planted coffee. There are two field-level characteristics
210 we consider to distinguish it from rubber: i) there is a checkboard-like pattern from the holes

211 dug for the coffee trees (particularly for sun coffee) and ii) newly planted coffee is often
212 fertilized. We hypothesize that our GLCM texture variables could help to contextualize the
213 surroundings of the newly planted coffee to better distinguish cleared rubber, newly planted
214 coffee and other bare soil. We draw from nitrogen management monitoring literature to
215 hypothesize that fertilization and soil properties associate with basaltic soils (reddish-brown)
216 can be detected through the visible band remote sensing (Blaes et al., 2016).

217

218 *On the separability of sun coffee and intercropped coffee:*

219 The plot characteristics of sun and intercropped coffee differ in the following ways (non-
220 exclusively) in which they would be distinguishable with the sensors and features used in our
221 study: i) higher moisture (less evapotranspiration) in intercropped coffee, ii) thicker canopy
222 and ground cover (rather than bare soil), and iii) “rougher” or more textured canopy for
223 intercropped coffee (Assefa and Gobena, 2019; Padovan et al., 2018; Siebert, 2002).

224 Sentinel-2 swir bands and Sentinel-1 bands are both sensitive to water and would entail that
225 intercropping has a higher reflectance and backscatter, for S2 and S1, respectively (Figure
226 S2 & S3). S1 GLCM texture features were designed primarily with distinguishing in-plot
227 canopy texture between the two coffee production systems. This drove our choice of window
228 sizes (further explained in Section 3.3).

229

230 3.1. Remote Sensing Data

231 In our multi-sensor approach, three remote sensing data types – optical data, SAR data and
232 topographic information – were integrated as predictors for the coffee classification. We used
233 10m-60m optical Sentinel-2 (S2) Surface Reflectance (SR), 10m SAR C-band Sentinel-1
234 (S1) Ground Range Data (GRD), and topographic Shuttle Radar Topographic Mission
235 (SRTM) 30m DEM data, accessed on GEE platform (Copernicus, retrieved: 11-12-2019; Farr
236 et al., 2007; Gorelick et al., 2017). It was key to include 10m resolution optical and radar in
237 this smallholder landscape as it allows for distinguishing cropping systems at the smallholder
238 plot-level. Additionally, SAR data added a temporally consistent data source in the cloudy

239 tropical and hilly region and the C-band wavelength at 5.6cm is more suitable than the L-
240 band sensor, typically used to monitor forest, due to coffee's smaller crown size.

241

242 Sentinel-2 SR images were accessed for 01 November, 2018 through 31 October, 2019
243 covering both wet and dry seasons (Table S1, Table S2). A filter was applied to consider
244 images with a cloudy pixel percent less than 10%, an estimated data attribute to all Sentinel
245 scenes. This was particularly important as Sentinel cloud masks are not yet as developed as
246 e.g. Landsat cloud masks. Using highly clouded scenes will likely result in cloud artefacts,
247 impacting the spectral signal.

248

249 Sentinel-1 GRD data were obtained for the same date range. We utilize data from vertical
250 transmit and vertical receive (VV) and vertical transmit and horizontal receive (VH)
251 polarization (as this is what is available in this region) and interferometric wide swath
252 acquisition mode (Table S1, Table S2). The Copernicus S1 GRD data is already multi-looked
253 (converted from slant range) and projected to ground level. The data made available through
254 GEE has been pre-processed in the Sentinel Application Platform (SNAP) to apply the orbit
255 file, perform thermal noise removal, radiometric calibration and terrain correction, using
256 SRTM30 (ESA- S1TBX Sentinel-1 Toolbox, accessed: 05-02-2021).

257

258 3.2. Reference Data & Classification Scheme

259 Reference data refers to all point data used to parameterize, train and test the classification.
260 These points were collected using Collect Earth (Bey et al., 2016) and Google Earth high-
261 resolution imagery from the year 2019 in two rounds: at the province level across Dak Lak,
262 and at the sub-province district level in Ea H'Leo (see Figure 1). This data collection was
263 facilitated by a field visit in summer 2019 where location points for different land cover
264 classes were collected using a handheld smart device. For both sets of reference data
265 (province and district level), we randomly sampled and labelled following the classification
266 scheme in Figure 2. If randomly sampled points fell in between classes or in a mixed area,


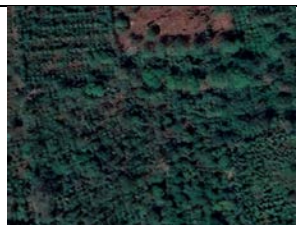

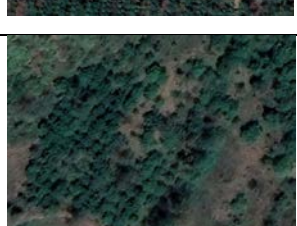


267 they were resampled within one km for all relevant classes. Additionally, iterative
268 opportunistic sampling was used to sample particularly from the coffee target classes and
269 cultivated vegetation (both annual and perennial crop) classes, the classes that are most
270 often confused with coffee (Figure 2). The Ea H'Leo set (600 points) was used to test and
271 select a subset of features to use in the classifier at the full province level, in a calibration
272 and feature reduction phase. The Dak Lak dataset (~1000 points) was randomly split 70/30
273 into a train and test dataset for the random forest classifier, ensuring that at least 50 points
274 for each of our 9 classes were part of training dataset.






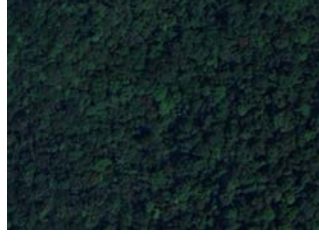

275

276 The reference data classification scheme was collected at the “lowest denominator,” most
277 detailed categorical level and aggregated as needed for each of the classifications (Table 1;
278 Bey et al., 2020). This modular scheme allowed for flexibility in re-grouping classes based on
279 the classification needs and application. For example, we use this dataset to classify a
280 detailed land cover map, targeting coffee sub-classes, and in a binary coffee/ non-coffee
281 map.

282

283 *Table 1.* Classification scheme, with example high-resolution imagery from Google Earth
 284 imagery for the reference data (points), and how it was aggregated for the detailed land
 285 cover map and binary classification scheme.

Reference scheme	Detailed land cover scheme	Binary classification scheme	Reference image from Google Earth
Sun coffee (coffee with an open canopy)	sun coffee	coffee	
Intercropped or other shade coffee	intercropped coffee	coffee	
Newly planted coffee (sparse)	newly planted coffee	coffee	
Other tree crop (including e.g. acacia, cashew)	partially vegetated	non-coffee	
Newly planted fruit or nut tree crop (sparse)	upland crop	non-coffee	
Upland crop	upland crop	non-coffee	

Shrubland	partially vegetated	non-coffee	
Low or no vegetation (including bare soil)	partially vegetated	non-coffee	
Mature rubber plantation	heavily vegetated or forested	non-coffee	
Clear or young rubber	upland crop	non-coffee	
Dry deciduous forest	partially vegetated	non-coffee	
Evergreen forest	heavily vegetated or forested	non-coffee	
Mixed forest	heavily vegetated or forested	non-coffee	

Wet crop (rice)	rice	non-coffee	
Built	built	non-coffee	
Water	water	non-coffee	

286

287

288 For the detailed land cover map, we aggregated non-target (non-coffee) classes that were
 289 most often confused in the calibration phase. This includes the aggregation of dry deciduous,
 290 other tree crop, and low vegetation, where our classifier is most likely confusing the low
 291 foliage deciduous forest with low or no vegetation particularly in the dry season. For the
 292 binary coffee map, the detailed land cover labels were reclassified as coffee or non-coffee.

293

294 3.3. Data Pre-processing

295 Each scene in the Sentinel-2 Surface Reflectance series were cloud masked using the GEE
 296 implemented cloudscore algorithm and shadow masked using temporal dark outlier mask
 297 (TDOM) (Housman et al., 2018; Schmitt et al., 2019). For each cloud and shadow masked
 298 S2 scene, a stack of spectral indices was calculated and appended, creating a collection of
 299 66 scenes with the 10 reflectance bands and 13 computed indices (Table S3). This collection
 300 was then split into dry season from 01 November, 2018 to 15 April, 2019 and wet season,
 301 from 01 May to 31 October, 2019. The median values from the 44 dry season scenes and 22
 302 wet season scenes were taken to create two seasonal image stacks from the S2 data (Figure

303 2). Although there are many ways to composite an image, we decided for the median due to
304 limited scenes in the wet season, where max or min values could be contaminated by cloud
305 and cloud shadow.

306
307 Our image search for the study area returned 90 ascending VV, 90 ascending VH, 60
308 descending VV, and 60 ascending VH scenes (Table S4). An initial variable importance
309 analysis (random forest) with the Ea H'Leo district reference set showed a consistently
310 higher importance for descending scenes, perhaps due to topography or the different pass
311 times of ascending and descending. A preliminary look at VV and VH backscatter also
312 showed a more defined signal between sun and intercropped coffee for VH (Figure S3).
313 Therefore, SAR-derived temporal statistics and texture features at the Dak Lak level were
314 only calculated for the descending scenes for both polarizations (VV & VH). First, spectral
315 temporal statistics were calculated for the VV descending and VH descending time series.
316 These metrics, including median, 25th and 75th percentile and standard deviation across the
317 time series of scenes, are often used for optical Landsat imagery in less cloudy regions, such
318 as in Hu et al., (2018); Müller et al., (2015); Pflugmacher et al., (2019). Yet such metrics are
319 not as effective in sparse time series, as is often the case for wet season optical data in the
320 tropics. S1 radar data, with its cloud non-dependence and dense time series (revisits roughly
321 ~6 days) allows us to leverage the added value information that temporal statistics can offer.

322
323 In addition to the S1 spectral temporal metrics, 8 Gray Level Co-occurrence Matrix (GLCM)
324 texture variables (Haralick et al., 1973) were calculated for the median composite of the
325 descending VH series using a 5x5 moving window, with a displacement of 1, and averaged
326 over four spatial orientations (Figure 2). After testing moving windows of size 3, 5, and 7 in
327 Ea H'Leo, a 5x5 pixel moving window was chosen to best capture the plot-level texture,
328 particularly between sun and intercropped coffee. S1 SAR textural information has been
329 shown to be particularly beneficial in heterogenous landscape (Mishra et al., 2019),
330 distinguishing between smallholder and large-scale plantations (Oon et al., 2019), but has

331 also been applied for agroforestry mapping, as is done for a cocoa landscape in Numbisi et
332 al., (2019).

333
334 The S2, S1 and topography image stacks were all prepared and combined into a single stack
335 in GEE. Although the random forest classifier has been assumed to deal well with high-
336 dimensional data, it has been shown that large numbers of correlated input features can
337 disadvantage the minority class (Waldner et al., 2019), especially when trying to capture
338 small proportion target classes (such as newly planted coffee). In order to reduce the 67
339 prepared features and multicollinearity, we applied a variance inflation factor (VIF). The full
340 feature stack was exported into R and a VIF: $\frac{1}{1-R^2}$, where R^2 is the coefficient of
341 determination, was computed for each of the 67 features, by sampling at the Ea H'leo
342 reference points. Any feature with a VIF higher than 10 was removed, which is often
343 considered the rule of thumb (O'Brien, 2007). This step resulted in 22 features, representing
344 all five types: S2 wet and dry season composites, S1 spectral temporal metrics, S1 texture
345 variables, and SRTM topographic variables (Table 2). These features were the input for the
346 random forest classifier.

347

348 3.4. Calibration

349 Before running our final classifications, we calibrated our model at the sub-province level (Ea
350 H'leo). Calibration entailed using the Ea H'leo reference data and our full feature set (67
351 features) as input into an initial classifier, inspecting confusion between classes, and variable
352 importance metrics. The calibration phases tested multiple land cover classification schemes
353 and informed the aggregation of classes that would best allow for the targeting of coffee. For
354 example, natural forest and mature rubber plantations had high confusion most likely due to
355 their high planting density and similarity in height. Additionally, in the north of Dak Lak, dry
356 deciduous forest, low or no vegetation and "other tree crops," which in this area is primarily

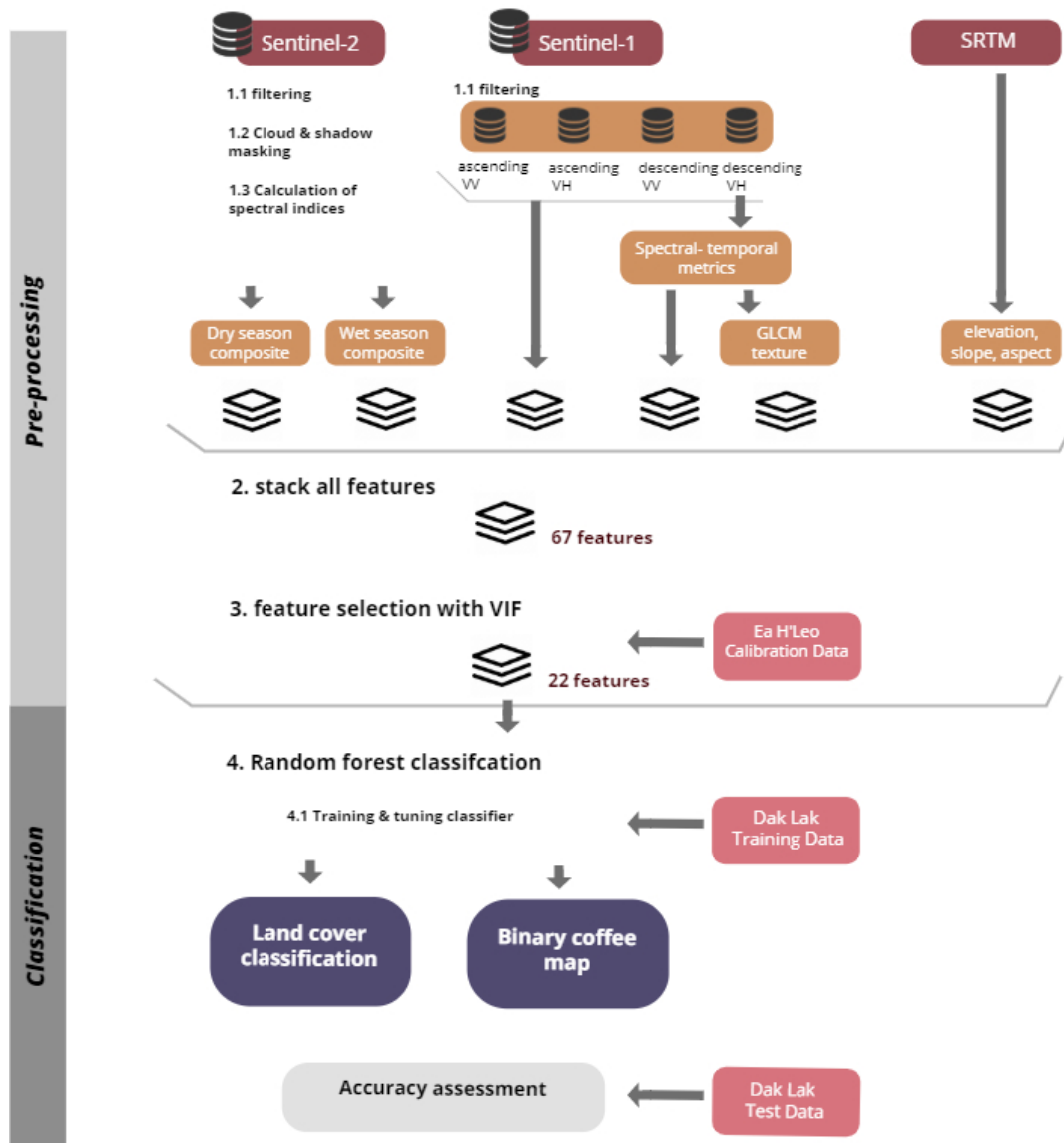
357 acacia, were being confused, most likely due to their similarities in low foliage during the dry
358 season.

359

360 The variable importance analysis for Ea H'Leo aligned with the variable importance for Dak
361 Lak. For example, ndti (normalized tillage index, a swir1 and swir2 normalization) and
362 elevation maintained their relative importance in both Ea H'Leo and Dak Lak, across multiple
363 runs. Lastly, in the calibration phase, we also reduced our feature set, using VIF (detailed in
364 3.3 Data pre-processing). This reduce collinearity between features (and minimizes OOB_e),
365 allowing for a more stable re-application of our method at a higher scale and in other areas.

366

367



368

369 *Figure 2.* Methods workflow showing data used, pre-processing steps and classification

370 inputs and outputs.

371

372 *Table 2.* Features inputted into the classifier after a feature reduction (using a Variable
 373 Inflation Factor method). The features are grouped in the 5 categories: Sentinel-2 derived
 374 features in the dry season; Sentinel-2 derived features in the wet season, Sentinel-1
 375 spatiotemporal metrics (temporal statistics), Sentinel-1 texture metrics, and DEM-derived.

Category	Features included (22)
S2- dry season	blue nir Green Chlorophyll Vegetation Index (GCVI) Modified Crop Residue Cover (MCRC) Normalized Difference Tillage Index (NDTI)
S2- wet season	blue nir swir2 MTCI GCVI MCRC
S1 SAR (including spatiotemporal metrics)	VV asc median ratio VV:VH desc standard dev. VV desc 75 th percentile VV desc 75 th percentile VH desc
S1 SAR- texture metrics	GLCM correlation GLCM sum variance GLCM angular second moment (ASM)
DEM-derived metrics	elevation slope aspect

376

377 3.5. Classification

378 In order to create i) a detailed land cover map with coffee production systems specified and
379 ii) a binary coffee mask, both at 10m resolution, two random forest classifiers were
380 implemented in Google Earth Engine. Random forest (RF) is a machine learning algorithm
381 that uses a decision tree-based ensemble and bootstrap aggregation (bagging) of training
382 data, described in the landmark paper (Breiman, 2001). RF is often used for remote sensing
383 classification problems for its robustness compared to individual models, relative resistance
384 to noise, ability to handle high-dimensionality, and ease of parameterization (Belgiu and
385 Drăguț, 2016; Hengl et al., 2018). There are three main user-defined hyperparameters for RF
386 models: number of trees, number of variables per split and maximum number of splits.
387 Number of trees is the number of individual models in the ensemble, or number of decision
388 trees in the “forest.” Number of variables per split (or node on a decision tree) is a restriction
389 from 1 to the total number of features, that can be used to create the most separation at any
390 specific node. If the number of variables per split is less, this creates more variation between
391 the trees. And lastly, the maximum number of splits restricts the depth of the individual trees.
392 Theoretically, the hyperparameter values shouldn’t strongly influence the outputs, however
393 practically, they need to be tuned (Scornet, 2017). The hyperparameters, number of trees
394 and variables per split, were tuned using the out-of-bag error (OOBe) and step-wise test runs
395 of all reasonable combinations (Table S5, Table S6). In GEE, we set bagging to 65% for the
396 calculation of the internal OOBe used to tune the random forest model. Based on the tuning,
397 we ran both the detailed land cover and binary classifiers with 2000 trees and 2 variables per
398 split. We used the default for maximum depth of trees, unrestricted.

399
400 A random sub-selection of 70% of the Dak Lak reference data (Section 3.2) was used to train
401 the random forest classifier, each training point could be thought of as a vector with
402 associated values sampled from the 22 features, selected using VIF (Section 3.3). The
403 detailed land cover map being trained on a 9-class schematic specified in the second column
404 of Table 1 and the coffee mask being trained on with a binary coffee / non-coffee scheme.

405
406 In addition to the traditional accuracy assessment matrix, we would refer to another metric:
407 quantity disagreement and allocation disagreement, as proposed by Pontius and Millones
408 (2011) in substitution of kappa. Pontius and Millones argue that overall accuracy (agreement)
409 and kappa provide only a positive evaluation and do not give information on the certainty of
410 how a classification *does not* perform. Quantity disagreement can be defined as the
411 differences between the reference data and the classification attributing to an imperfect
412 match in the proportion of the categories. Allocation disagreement is defined as the
413 differences in geographic spread of pixels between reference and classification. The “total
414 disagreement,” or the percentage of mismatch, between the reference and classification is
415 the sum of the quantity and allocation disagreement.

416
417 For the detailed land cover classification, we also carried out sensitivity analysis by running
418 our classifier with our feature subsets (S1 spectral temporal metrics, S1 GLCM texture
419 features, S2 wet season, S2 dry season, topographic) and various combinations of these
420 subsets.

421

422 4. Results

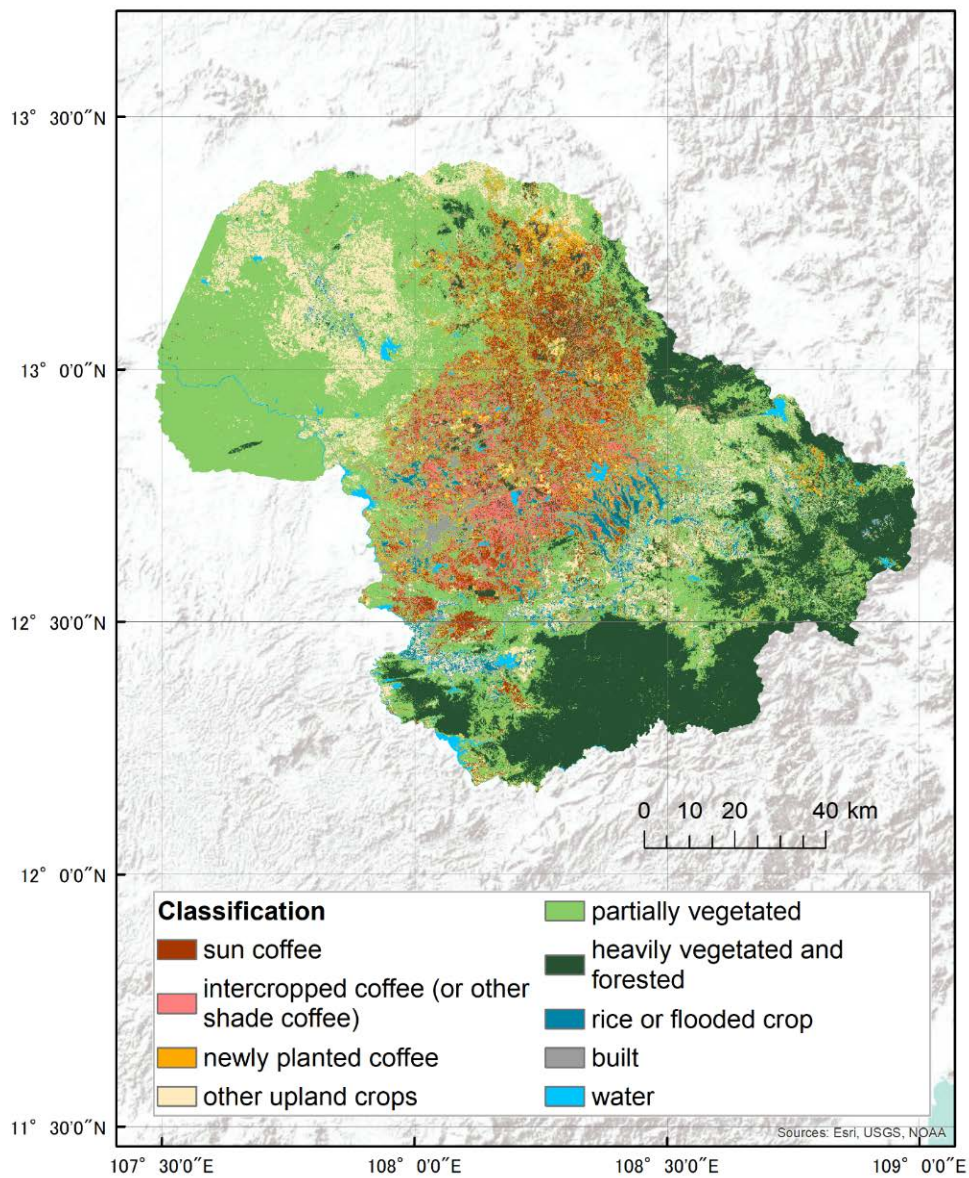
423 4.1. Detailed Land Cover Map

424 The detailed land cover classification offers a method for employing open 10m Sentinel
425 optical and radar data to characterize plot-level production system for coffee within a highly
426 heterogeneous landscape, while also covering a province-level area of 13,000 km².

427
428 Our classified land cover map shows coffee plantations clustered in the middle stripe of Dak
429 Lak, in mid-range elevation (Figure 3, Figure 4D). Visually, intercropping and other shade
430 systems are concentrated around Buon Ma Thuot, the Central Highland's "coffee capital"
431 (Figure 4E). New coffee plantations are often on increasing elevations, with concentrations in
432 the Northeast in Ea H'Leo (Figure 4A) and a patch of new coffee landscape in M'Drak
433 (Figure 4B). The overall accuracy is 72.5% (Table 4), with user accuracies of 64.5%, 56.0%,
434 and 70.8% for sun, intercropped and newly planted coffee respectively. The classifier's most
435 common confusion is between sun and intercropped coffee, as expected. We also find a
436 slight over-classification of all coffee classes (and agricultural land) at the expense of the
437 partially vegetated class.

438
439 Figure 4 also highlights how our classification captures patterns of high heterogeneity within
440 the landscape. It is common that neighboring plots of sun, intercropped and newly planted
441 coffee are often patchworked, along with other annual and perennial crops or because
442 farmers plant coffee gardens next to their houses. Our classifier was able to represent these
443 intricacies of the landscape with good agreement of this challenging task. Our classification
444 and reference data had a quantity difference of 6.2% and an allocation difference of 21.3%,
445 with the majority of the disagreement or error attributed to spatial mismatch, primarily in the
446 partially vegetated class (Table 5).

447



448

449 *Figure 3. Map of detailed land cover classification for Dak Lak at 10-m resolution.*

450

451

452

453 *Table 4. Accuracy assessment for detailed land cover classification.**detailed land cover classification*

<i>test data</i>	<i>detailed land cover classification</i>										count	user accuracy
	sun	intercropped	newly planted	upland crop	partially vegetated	heavily vegetated	rice	built	water			
sun	20	8	0	1	2	0	0	0	0		31	0.645
intercropped	8	14	0	0	2	0	0	1	0		25	0.560
newly planted	2	0	17	3	1	0	1	0	0		24	0.708
upland crop	1	0	4	25	4	0	3	0	0		37	0.676
partially vegetated	4	3	3	10	74	8	2	1	2		107	0.692
heavily vegetated	1	2	0	0	4	33	0	0	0		40	0.825
rice	0	0	2	4	0	1	15	0	0		22	0.682
built	0	0	0	0	0	0	0	18	0		18	1.000
water	0	0	0	0	0	0	1	0	19		20	0.950
count	36	27	26	43	87	42	22	20	21		overall accuracy	0.725
producer accuracy	0.556	0.519	0.654	0.581	0.851	0.786	0.682	0.900	0.905		kappa	0.675

454

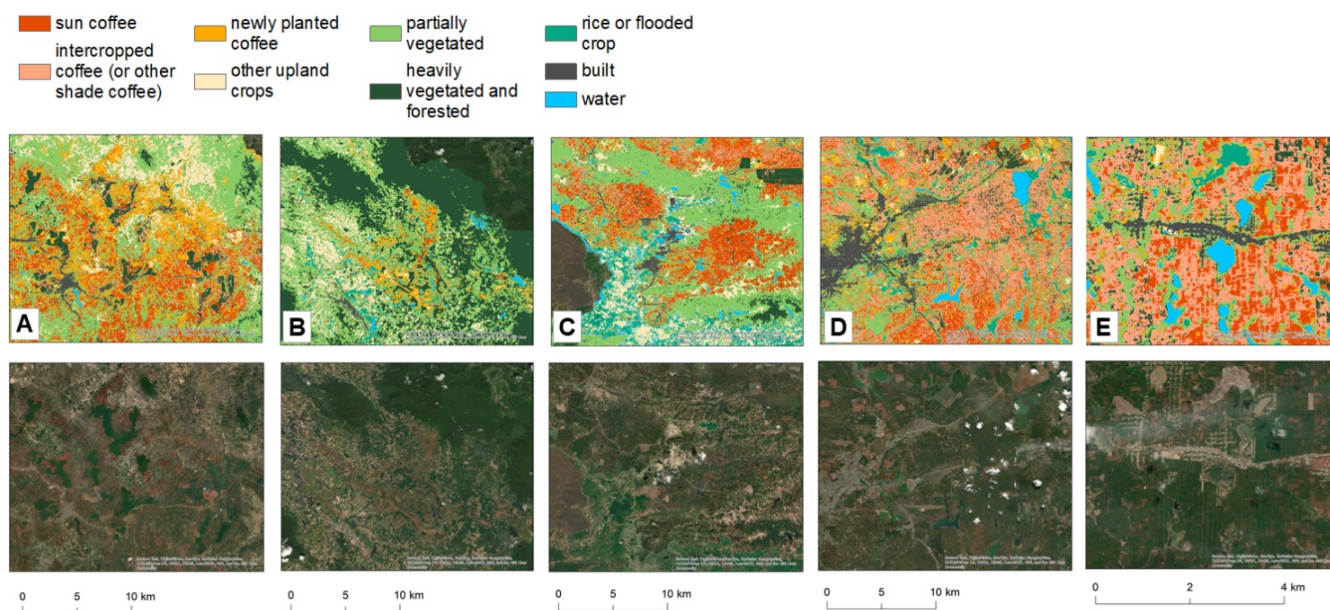
455

456 *Table 5. Overall disagreement metrics from Pontius and Millones (2011) for the detailed land*
 457 *cover map and the binary map. Agreement (or persistence) is equivalent to overall accuracy*
 458 *and total disagreement is the inverse.*

	Agreement or Persistence	Commission or Loss	Omission or Gain	Total Disagreement	Quantity Disagreement	Allocation Disagreement
detailed land cover map	0.725	0.275	0.275	0.275	0.062	0.213
binary map	0.886	0.114	0.114	0.114	0.071	0.043

459

460



461

462 *Figure 4.* Closer look at the detailed land cover map in order to highlight specific landscape
 463 processes being captured, along with the corresponding satellite images: A) concentration of
 464 many new coffee plots, in a sun coffee and rubber landscape in Ea H'Leo, B) establishment
 465 of newly planted coffee in M'Drak (Eastern-most district), C) area dominated by sun coffee in
 466 Krong Ana, D) high concentration of intercropped or shade coffee near Buon Ma Thuot, E)
 467 zoomed in view near Buon Ma Thuot, an area of mixed sun and intercropped plots.

468

469

470 *Table 6.* The performance of detailed land cover model with inputs of feature subsets and
 471 combination of subsets. The 5 subsets are Sentinel-2 (S2) dry season composite, S2 wet
 472 season composite, Sentinel-1 (S1) spatiotemporal metrics, S1 Gray Level Occurrence Matric
 473 (GLCM) texture features and topographic features (SRTM). Overall accuracy (OA) and out-
 474 of-bag error (OOBe) are presented.

	Number of features	OA	OOBe
			475
S2 dry only	22	0.65	0.40
S2 dry + wet	44	0.70	0.34
S2 all + SRTM	47	0.73	0.33
S1 spectral temporal	12	0.40	0.54
S1 GLCM	8	0.32	0.67
S1 all	20	0.46	0.52
S2 all + SRTM + S1 spectral temporal	59	0.74	0.30
S2 all + SRTM + S1 GLCM	55	0.73	0.32
all bands (full set)	67	0.67	0.31
reduced set (presented in Figure 4, Table 4)	22	0.73	0.28

476

477 Similar to other LULC mapping studies, optical seasonal composite gives an added
 478 information to the classifier, increasing both the overall accuracy and decreasing the OOBe
 479 (Table 6; Jin et al., 2019; Nguyen et al., 2019; Poortinga et al., 2019; Spracklen and
 480 Spracklen, 2021). While neither S1 subset performs well on its own, in combination with S2,
 481 the accuracy increases. The OOBe is higher in the model runs including GLCM texture,
 482 which may be due to the fact that some GLCM features are highly correlated (Haralick et al.,
 483 1973). Nevertheless, the inclusion of GLCM with optical and topographical information still
 484 increases accuracy and decreases OOBe.

485

486 4.2. Binary Coffee / Non-coffee Map

487 The binary coffee classification has an overall accuracy of 88.6% and a user accuracy for the
488 coffee class of 89.4% (Table 7). The binary map was targeted with applications as a crop
489 mask, since it is relatively uncommon to find one for tree crop at such a high spatial
490 resolution with some degree of certainty (Inglada et al., 2015). This is highlighted in Figure 5,
491 which shows a comparison of our coffee map (A) and other coffee maps (B-D) with coverage
492 of Dak Lak.

493
494 Figure 5 helps to visualize the trade-off between spatial resolution, coverage, and information
495 depth. For example, the Japanese Aerospace Exploration Agency (JAXA) land cover dataset
496 (Figure 5B), offers a 10m spatial resolution for all of Vietnam but focuses on a rather general
497 land cover scheme, without a specific coffee class. In the JAXA dataset, coffee crop is
498 aggregated with other tree crops into the class “orchards.” A MODIS-derived dataset of
499 “boom crops” (e.g. primarily rubber and other tree crops) in Mainland Southeast Asia, offers
500 information on coffee at 250m resolution (Figure 5C). Our binary classification shows visual
501 agreement with Figure 5C in terms of spatial distribution. Figure 5D shows a global gridded
502 dataset on production area for FAO crops, where national and other administrative statistics
503 are aggregated and re-distributed to the grid-cell level (Monfreda et al., 2008). In order to
504 create the map shown in Figure 5D, cells with less than 1% of area covered by coffee were
505 filtered out. It is noteworthy that no grid cell in Dak Lak had more than 3% area covered by
506 coffee, according to the Monfreda dataset. The difference in spatial distribution between
507 Figure 5A and 5D highlights the difficulties in scaling information on landscape dynamics to
508 the global level.

509
510 With a producer accuracy for coffee of 66.3% in our detailed land cover map, the difference
511 between the user and producer accuracy implies an over-assigning of pixels to coffee. The
512 reference data was roughly proportional to land cover proportion for the binary map, as we
513 changed the classification scheme without reducing the number of points (from a random

514 sampling). As such, there were many more non-coffee training points compared to coffee
 515 training points and the over-assigning was unexpected. This is perhaps represented in the
 516 quantity and allocation disagreement, as quantity disagreement is higher than the allocation
 517 disagreement, at 7.1% and 4.3% respectively (Table 5).

518

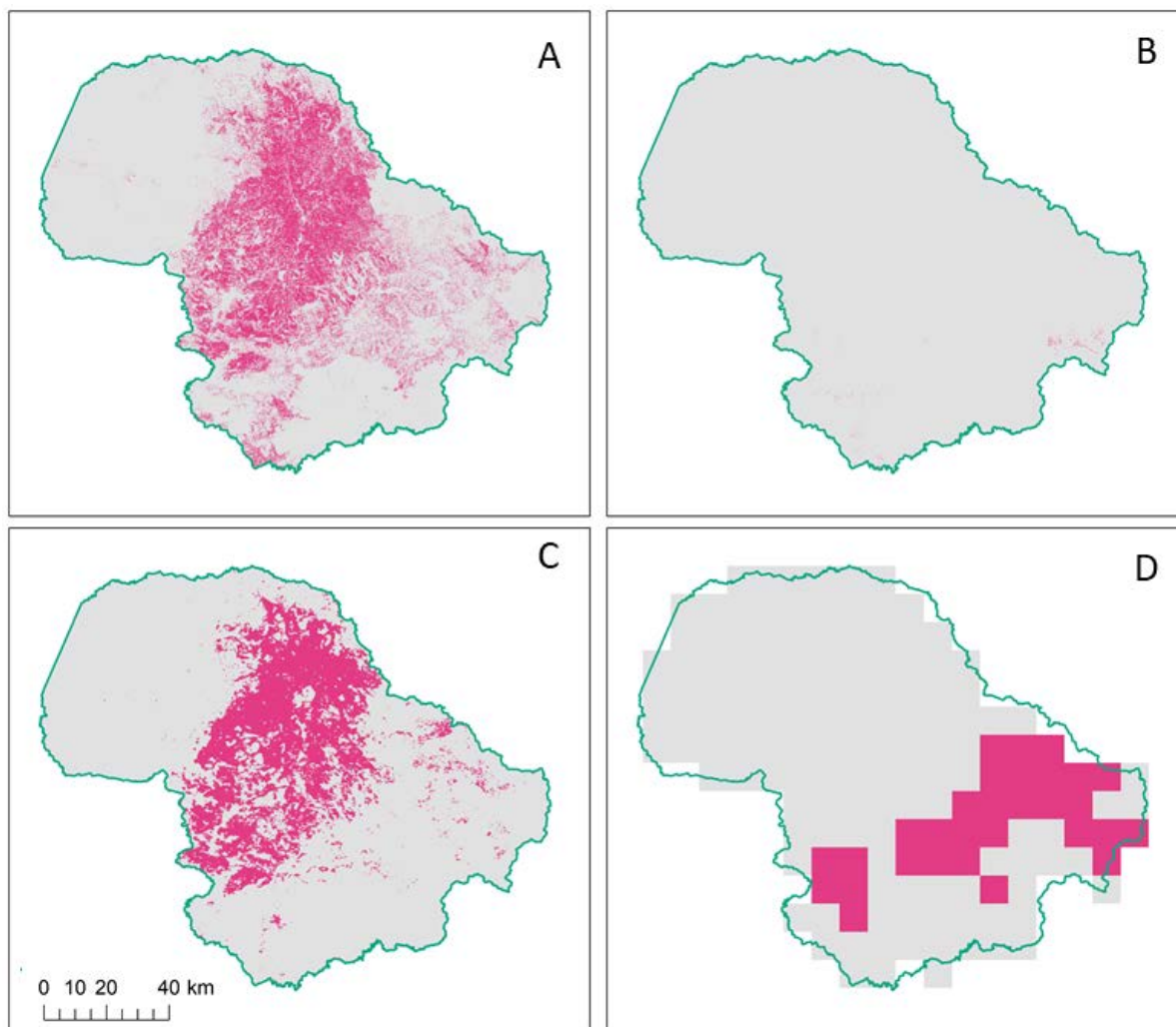
519

520 *Table 7. Accuracy assessment for binary classification.*

	non-coffee	coffee		count	user accuracy
non-coffee	228	30		258	0.884
coffee	7	59		66	0.894
count	235	89		overall accuracy	0.886
producer accuracy	0.970	0.663		kappa	0.689

521

522



523
 524 *Figure 5.* Comparison of A) the binary coffee map from this study; B) the orchard class from
 525 the 2017 JAXA Land cover map (10m), derived from S2, Landsat 7 & 8, ALOS/AVNIR-2,
 526 PALSAR, and SRTM (Duong et. al., 2018); C) Hurni and Fox's (2018) coffee class from their
 527 2014 boom crop mapping in Mainland Southeast Asia (250m), MODIS-derived; D) Monfreda
 528 et al., (2008) "fraction of harvested area," with a threshold of more than 1% coffee area
 529 harvested, disaggregated at the 5' (~10km) grid cell from agricultural statistics for 2000.

530

531

532 5. Discussion

533 The method presented here builds on large-scale, crop-specific mapping using the open
 534 Sentinel asset, advancing geospatial methodology on mapping coffee as a complex target
 535 and generating plot-level thematic information within a heterogenous landscape. Most other

536 large-scale Sentinel-based crop type mapping (Defou, 2019; Griffiths et al., 2019; Jin et al.,
537 2019) targets annual crops, such as maize or wheat. We delve into the large-scale mapping
538 of a tree crop, more along the lines of Poortinga et al. (2019), who mapped oil palm and
539 rubber in a cross-border protected area between Myanmar & Thailand. To our knowledge,
540 the work we present here is a first attempt at mapping coffee at the fine spatial resolution and
541 large geographic scales using Sentinel data.

542
543 The integration of both Sentinel-2 and Sentinel-1 in crop type mapping is still being
544 developed. The default is to rely solely on optical sensors; most work piloting the
545 combination of optical and SAR Sentinel data for crop type mapping is carried out on a
546 smaller geographic footprint (Denize et al., 2018; Sun et al., 2019). Nevertheless, recent
547 studies have started to focus on crop-specific mapping combining these two data streams at
548 regional to national scales (Jin et al., 2019; Poortinga et al., 2019). We contribute to this line
549 of research for mapping coffee production systems. As demonstrated in Jin et al., (2019) and
550 Poortinga et al., (2019), Sentinel-1 data has the added advantage of non-reliance on cloud-
551 free days, allowing for a temporally constant information source to supplement optical data,
552 especially in the cloudy tropics and sub-tropics. For coffee mapping or other lower biomass
553 or sparse tree crops, C-band data (e.g. Sentinel-1 SAR), with its smaller wavelength of 3 –
554 5cm, is better suited compared to higher wavelength L-band data, often used for forest
555 mapping.

556
557 As emphasized by Hunt et al. (2020), it is not common that coffee maps offer
558 characterization or sub-plot information on the production system or age of coffee stand. We
559 build off of the work using remote sensing to spatially characterize coffee production systems
560 (Cordero ~~Saetho~~ and Sader, 2003) and coffee age classes (Chemura et al., 2017; Chemura and
561 Mutanga, 2016) by developing a method that allows implementation at larger geographic
562 scale. This was enabled by i) open and easily accessible 10m Sentinel data, ii) GEE's cloud
563

564 computing infrastructure, and iii) inclusion of a diverse set of features: seasonal information
565 derived from optical imagery, radar temporal metrics, radar texture information and
566 topographic information. The first two points speak to openly available research resources
567 and infrastructure and the last speaks to a diversity of input features for representation of a
568 diverse landscape. We conclude that each set of features brings something specific to the
569 classifier's ability to separate classes. This is supported by a feature importance not
570 dominated by a specific feature, with all 22 features used in the classifier contributing to the
571 overall accuracy (*Figure S4*). For example, we theorize that the use of texture metrics was
572 particularly helpful in distinguishing between "textured" intercropping or other shade systems
573 and homogeneous sun plantations that occur adjacent to each other. And according to a
574 feature importance, the wet season SWIR2 band and the Normalized Difference Tillage
575 Index, a ratio index between SWIR1 and SWIR2, had the highest contribution to accuracy
576 (although not by a wide margin). This could be indicative of the importance of water regimes,
577 such as irrigation schedule, or soil signals, such as background soil from less densely
578 planted coffee, as SAR and SWIR are sensitive to water and soil signals.

579
580 In other smallholder landscapes it has been shown that that moderate resolution sensors,
581 such as Landsat (30m), offer an advantage over MODIS (250m) in identifying cropping
582 patterns in a Central Indian smallholder landscape (Jain et al., 2013), whereas very high-
583 resolution Planet data (of 3 – 5cm) allows for sub-plot crop monitoring at a farm in Southern
584 Brazil (Breunig et al., 2020). Our results fit in between these two works, presenting
585 information on the plot-level production system with a 10m resolution at a landscape scale.
586 This introduces a specific advantage over the previous work that cover Dak Lak (*Figure 5*).
587 Only one other work with coverage of Dak Lak produced a map explicitly including coffee and
588 did so using MODIS's 250m resolution as part of a mapping effort targeting rubber in South
589 East Asia (Hurni and Fox, 2018; *Figure 5c*). While JAXA produced a multi-sensor 10m land
590 cover map for Vietnam, coffee was not a separate class, and was aggregated into "orchard,"

591 defined as the intentional planting of trees or shrubs, which as a class did not perform well in
592 Dak Lak (Duong et al., 2018).

593
594 This first mapping of “full coverage” coffee production styles, intercropped and newly planted
595 coffee respectively, is useful in many applications. Information on where coffee is being re-
596 planted or planted for the first time, represented by our class “newly planted coffee,” can aid
597 in agricultural planning and monitoring deforestation (although both entail knowledge of the
598 past land cover, e.g. through time series analysis, which will be mentioned later in the
599 Discussion). Even though newly planted coffee is also confused with other agricultural land
600 (primarily cleared rubber) and our classifier slightly over-estimates newly planted coffee, it is
601 still a best-effort at addressing the two above-mentioned processes in the region. As a large
602 percentage of coffee trees in the region are aging, 33% are 15-20 years and 31% are over
603 20 years, local governments are targeting replantation programs, such as Decision No.
604 2729/QD-UBND from the People’s Committee of Dak Lak (Hung Anh et al., 2019). The map
605 and method presented here could offer one way of tracking progress, particularly in remote
606 areas. Additionally, newly planted coffee in regions that are otherwise primarily natural
607 vegetation or forest can give an indication for forest conversion, complementing prior work on
608 forest frontiers and agricultural dynamics in the Central Highlands (Bourgoin et al., 2020;
609 Meyfroidt et al., 2013; Phuc and Tran, 2014).

610
611 The spatial overview of implementation of agroforestry practices, represented by our class
612 “intercropping,” can i) assist in monitoring of sustainability certification and ii) complement
613 climate adaptation monitoring: two fields where monitoring is overwhelmingly undertaken
614 through household surveys. It is also the novelty of our classification that we attempt to
615 create spatially continuous dataset of information that is often collected and available at a
616 point or clustered level. There are limitations in the producer accuracies of sun and
617 intercropped coffee, primarily due to confusion between the two (as opposed to confusion
618 with other classes). Nevertheless, a remote sensing effort at tracking coffee production

619 systems is especially pertinent in hilly coffee regions, where field mapping is tricky due to
620 remoteness and steep terrain of coffee growing areas and remote sensing can offer an
621 information base layer for tracking sustainability and climate adaptation implementation. For
622 example, we hypothesize that the visual hot spot of intercropping close to Buon Ma Thuot
623 (Figure 4D &4E) could be attributed to the cluster of coffee companies, universities and
624 research institutes on coffee that are supporting implementation of sustainable practice in
625 coffee production including not only intercropping, but management of inputs, access to
626 credit among other factors.

627

628 We present a method based on the landscape and agroecological characteristics in Dak Lak,
629 however our approach was designed to scale from the district level, with calibration in Ea
630 H'Leo, to the province level, in Dak Lak. Particularly, feature reduction through VIF was
631 implemented to reduce overfitting, potentially allowing a better re-application or extrapolation
632 of our method in similar areas. With similar agroecological characteristics through the
633 Vietnamese Central Highlands, we imagine our feature set would perform well in neighboring
634 coffee growing landscapes. In order to generalize our approach to other coffee growing
635 regions, the optical seasonal composites would need to be adapted for other climates, and
636 may depend on the number of seasons per year as well as onset, cessation and precipitation
637 distribution. Using a similar approach, Kelley et al. (2018) maps coffee in a region of
638 Nicaragua which has three seasons and the primary coffee production system is shade or
639 traditional coffee. We hypothesize that our approach can be transferred to another climate
640 conditions and coffee production systems, by changing the region-specific features, but the
641 general transferability is not yet tested.

642

643 Tree crops are often completely excluded or have a high uncertainty in remote sensing
644 based mapping (Fritz et al., 2011; Inglada et al., 2015; See et al., 2015). While our model
645 targets coffee, we drew from mapping literature on similar tree crops: shade cocoa, coconut,
646 rubber, and oil palm. While separating tree crop from surrounding land cover such as forest

647 and other agriculture land, we would emphasize, in continuation of previous work, the added
648 value of texture features in distinguishing landscape and cropping systems (Burnett et al.,
649 2019; Gao et al., 2015; Gomez et al., 2010; Liu and Chen, 2019; Numbisi et al., 2019). We
650 would also make the distinction between tree crops with a regular clearing rotation (such as
651 rubber) and fruit and nut trees (such as a coffee and cocoa), and between monoculture
652 dominated landscape, agroforestry dominated landscapes, and mixed monoculture and
653 agroforestry. Aspects of our feature selection and processing, particularly the combination of
654 multiple sensor and feature permutations, could be adapted specifically for fruit and nut tree,
655 in mixed smallholder landscapes (Table 6). The adoption would need to be context specific in
656 terms of seasonal characteristics and confounding land cover and crops.

657
658 The dataset we developed can serve as a baseline for a future time-series study. This could
659 entail change detection for non-coffee (such as forest) to coffee, sun coffee to intercropped
660 coffee, or the identification of replantation or abandonment of coffee. All of these land cover
661 pathways can add a temporal dimension to the applications of deforestation and
662 sustainability in coffee production. These land cover pathways would be extremely useful in
663 building a timeline of a spatial continuous proxy for, e.g. forest vulnerability as done in
664 Meyfroidt et al., (2013), or sustainable growing or climate adaptation proxies, an emerging
665 interdisciplinary field between spatial sciences and sustainability science.

666

667 6. Conclusion

668 The work here offers a scalable method for mapping coffee production systems, and more
669 broadly plantation and agroforestry systems, as well as presents a coffee map for a major
670 world coffee-growing region, Dak Lak, Vietnam. In addition to benefiting from open 10m
671 Sentinel-2 optical data and Sentinel-1 radar data, our method demonstrates the added value
672 of heterogenous input features for a heterogenous landscape. Notably, cloud-independent
673 Sentinel-1 SAR time series and texture features complement the established seasonal
674 optical composites and SRTM topographic variables. The results present a binary coffee

675 mask, with an overall accuracy of 89.4%, and a 9-class land cover map in a first effort to
676 distinguish sun coffee, intercropped coffee and newly planted coffee, to broaden the
677 applications of remote sensing in deriving thematic agricultural information at finer spatial
678 scale.

679

680

681

682 Acknowledgment:

683 We are grateful to Pamela D. McElwee, Sonali Shukla McDermid, Tran Huu Nghi and
684 Nguyen Thi Quynh Thu and colleagues at Tropenbos International for their input during the
685 initial development of this research. This research is funded by a University of Delaware
686 Research Foundation grant awarded to PM. GM's doctoral research is funded by the Berlin-
687 Potsdam Research Network Geo.X.

688

689 Links to GEE script:

690 Pre-processing: <https://code.earthengine.google.com/268aad86925d374806d942635317d42c>

691 Classification: <https://code.earthengine.google.com/ee13aca08dd96f0ab0fe87f6c14dbdad>

692

693

694 7. References

- 695 Agergaard, J., Fold, N., Gough, K.V., 2009. Global-local interactions: socioeconomic and spatial
696 dynamics in Vietnam's coffee frontier. *Geogr. J.* 175, 133–145. <https://doi.org/10.1111/j.1475-4959.2009.00320.x>
697
- 698 Amarasinghe, U.A., Hoanh, C.T., D'haeze, D., Hung, T.Q., 2015. Toward sustainable coffee
699 production in Vietnam: More coffee with less water. *Agric. Syst.* 136, 96–105.
700 <https://doi.org/10.1016/j.agry.2015.02.008>
- 701 Assefa, A., Gobena, A., 2019. Review on Effect of Shade Tree on Microclimate, Growth and
702 Physiology of Coffee Arabica: In case of Ethiopia. *Int. J. For. Hortic.* 5.
703 <https://doi.org/10.20431/2454-9487.0503004>
- 704 Belgiu, M., Drăguț, L., 2016. Random forest in remote sensing: A review of applications and future
705 directions. *ISPRS J. Photogramm. Remote Sens.* 114, 24–31.
706 <https://doi.org/10.1016/j.isprsjprs.2016.01.011>
- 707 Bey, A., Sánchez-Paus Díaz, A., Maniatis, D., Marchi, G., Mollicone, D., Ricci, S., Bastin, J.-F., Moore,
708 R., Federici, S., Rezende, M., Patriarca, C., Turia, R., Gamoga, G., Abe, H., Kaidong, E.,
709 Miceli, G., 2016. Collect Earth: Land Use and Land Cover Assessment through Augmented
710 Visual Interpretation. *Remote Sens.* 8, 807. <https://doi.org/10.3390/rs8100807>
- 711 Bourgoin, C., Oszwald, J., Bourgoin, J., Gond, V., Blanc, L., Dessard, H., Phan, T.V., Sist, P.,
712 Läderach, P., Reymondin, L., 2020. Assessing the ecological vulnerability of forest landscape
713 to agricultural frontier expansion in the Central Highlands of Vietnam. *Int. J. Appl. Earth Obs.*
714 *Geoinformation* 84, 101958. <https://doi.org/10.1016/j.jag.2019.101958>
- 715 Brandt, J., Stolle, F., 2021. A global method to identify trees inside and outside of forests with
716 medium-resolution satellite imagery. *Remote Sensing* 18.
- 717 Breiman, L., 2001. Random Forests. *Machine Learning*.
- 718 Breunig, F.M., Galvão, L.S., Dalagnol, R., Santi, A.L., Della Flora, D.P., Chen, S., 2020. Assessing the
719 effect of spatial resolution on the delineation of management zones for smallholder farming in
720 southern Brazil. *Remote Sens. Appl. Soc. Environ.* 19, 100325.
721 <https://doi.org/10.1016/j.rsase.2020.100325>
- 722 Burnett, M.W., White, T.D., McCauley, D.J., De Leo, G.A., Micheli, F., 2019. Quantifying coconut palm
723 extent on Pacific islands using spectral and textural analysis of very high resolution imagery.
724 *Int. J. Remote Sens.* 40, 7329–7355. <https://doi.org/10.1080/01431161.2019.1594440>
- 725 Byrareddy, V., 2020. Win-win_ Improved irrigation management saves water and increases yield for
726 robusta coffee farms in Vietnam. *Agric. Water Manag.* 12.
- 727 Chemura, A., Mutanga, O., 2016. Developing detailed age-specific thematic maps for coffee (*Coffea*
728 *arabica*) in heterogeneous agricultural landscapes using random forests applied on Landsat 8
729 multispectral sensor. *Geocarto Int.* 32, 759–776.
730 <https://doi.org/10.1080/10106049.2016.1178812>
- 731 Chemura, A., Mutanga, O., Dube, T., 2017. Integrating age in the detection and mapping of
732 incongruous patches in coffee (*Coffea arabica*) plantations using multi-temporal Landsat 8
733 NDVI anomalies. *Int. J. Appl. Earth Obs. Geoinformation* 57, 1–13.
734 <https://doi.org/10.1016/j.jag.2016.12.007>
- 735 Clerici, N., Valbuena Calderón, C.A., Posada, J.M., 2017. Fusion of Sentinel-1A and Sentinel-2A data
736 for land cover mapping: a case study in the lower Magdalena region, Colombia. *J. Maps* 13,
737 718–726. <https://doi.org/10.1080/17445647.2017.1372316>

- 738 Copernicus Sentinel-1 & Sentinel-2 data [2018-2019]. Retrieved from Google Earth Engine [12-11-
739 2019], processed by ESA.
- 740 Cordero-Sancho, S., Sader, S.A., 2007. Spectral analysis and classification accuracy of coffee crops
741 using Landsat and a topographic-environmental model. *Int. J. Remote Sens.* 28, 1577–1593.
742 <https://doi.org/10.1080/01431160600887680>
- 743 DaMatta, F.M., Ronchi, C.P., Maestri, M., Barros, R.S., 2007. Ecophysiology of coffee growth and
744 production. *Braz. J. Plant Physiol.* 19, 485–510. [https://doi.org/10.1590/S1677-
745 04202007000400014](https://doi.org/10.1590/S1677-04202007000400014)
- 746 Dawson, I.K., Leakey, R., Clement, C.R., Weber, J.C., Cornelius, J.P., Roshetko, J.M., Vinceti, B.,
747 Kalinganire, A., Tchoundjeu, Z., Masters, E., Jamnadass, R., 2014. The management of tree
748 genetic resources and the livelihoods of rural communities in the tropics: Non-timber forest
749 products, smallholder agroforestry practices and tree commodity crops. *For. Ecol. Manag.*
750 333, 9–21. <https://doi.org/10.1016/j.foreco.2014.01.021>
- 751 De Beenhouwer, M., Aerts, R., Honnay, O., 2013. A global meta-analysis of the biodiversity and
752 ecosystem service benefits of coffee and cacao agroforestry. *Agric. Ecosyst. Environ.* 175, 1–
753 7. <https://doi.org/10.1016/j.agee.2013.05.003>
- 754 de Carvalho, A.F., Fernandes-Filho, E.I., Daher, M., Gomes, L. de C., Cardoso, I.M., Fernandes,
755 R.B.A., Schaefer, C.E.G.R., 2020. Microclimate and soil and water loss in shaded and
756 unshaded agroforestry coffee systems. *Agrofor. Syst.* [https://doi.org/10.1007/s10457-020-
757 00567-6](https://doi.org/10.1007/s10457-020-00567-6)
- 758 Defourny, P., 2019. Near real-time agriculture monitoring at national scale at parcel resolution_
759 Performance assessment of the Sen2-Agri automated system in various cropping systems
760 around the world. *Remote Sens. Environ.* 18.
- 761 Denize, J., Hubert-Moy, L., Betbeder, J., Corgne, S., Baudry, J., Pottier, E., 2018. Evaluation of Using
762 Sentinel-1 and -2 Time-Series to Identify Winter Land Use in Agricultural Landscapes. *Remote
763 Sens.* 11, 37. <https://doi.org/10.3390/rs11010037>
- 764 Duong, P., Trung, T., Nasahara, K., Tadono, T., 2018. JAXA High-Resolution Land Use/Land Cover
765 Map for Central Vietnam in 2007 and 2017. *Remote Sens.* 10, 1406.
766 <https://doi.org/10.3390/rs10091406>
- 767 ESA- S1TBX Sentinel-1 Toolbox. <http://step.esa.int> (accessed: 05-02-2021).
- 768 FAO. Food and Agriculture Organization of the UN. FAOSTAT Statistical Database. Rome, 1997.
769 <http://www.fao.org/faostat/en/#data> (accessed 20-01-21).
- 770 Fridell, G., 2014. Fair trade slippages and Vietnam gaps: the ideological fantasies of fair trade coffee.
771 *Third World Q.* 35, 1179–1194. <https://doi.org/10.1080/01436597.2014.926108>
- 772 Fritz, S., See, L., McCallum, I., Schill, C., Obersteiner, M., van der Velde, M., Boettcher, H., Havlík, P.,
773 Achard, F., 2011. Highlighting continued uncertainty in global land cover maps for the user
774 community. *Environ. Res. Lett.* 6, 044005. <https://doi.org/10.1088/1748-9326/6/4/044005>
- 775 Gaertner, J., 2017. Vegetation classification of Coffea on Hawaii Island using WorldView-2 satellite
776 imagery. *J. Appl. Remote Sens.* 11, 1. <https://doi.org/10.1117/1.JRS.11.046005>
- 777 Gao, T., Zhu, J., Zheng, X., Shang, G., Huang, L., Wu, S., 2015. Mapping Spatial Distribution of Larch
778 Plantations from Multi-Seasonal Landsat-8 OLI Imagery and Multi-Scale Textures Using
779 Random Forests. *Remote Sens.* 7, 1702–1720. <https://doi.org/10.3390/rs70201702>
- 780 Gomez, C., Mangeas, M., Petit, M., Corbane, C., Hamon, P., Hamon, S., De Kochko, A., Le Pierres,
781 D., Poncet, V., Despinoy, M., 2010. Use of high-resolution satellite imagery in an integrated

- 782 model to predict the distribution of shade coffee tree hybrid zones. *Remote Sens. Environ.*
783 114, 2731–2744. <https://doi.org/10.1016/j.rse.2010.06.007>
- 784 Gorelick, N., Hancher, M., Dixon, M., Ilyushchenko, S., Thau, D., Moore, R., 2017. Google Earth
785 Engine: Planetary-scale geospatial analysis for everyone. *Remote Sens. Environ.*
- 786 Griffiths, P., Nendel, C., Hostert, P., 2019. Intra-annual reflectance composites from Sentinel-2 and
787 Landsat for national-scale crop and land cover mapping. *Remote Sens. Environ.* 220, 135–
788 151. <https://doi.org/10.1016/j.rse.2018.10.031>
- 789 Grogan, K., Pflugmacher, D., Hostert, P., Kennedy, R., Fensholt, R., 2015. Cross-border forest
790 disturbance and the role of natural rubber in mainland Southeast Asia using annual Landsat
791 time series. *Remote Sens. Environ.* 169, 438–453. <https://doi.org/10.1016/j.rse.2015.03.001>
- 792 Ha, D.T., Shively, G., 2007. Coffee Boom, Coffee Bust and Smallholder Response in Vietnam's
793 Central Highlands. *Rev. Dev. Econ.* 15. <https://doi.org/10.1111/j.1467-9361.2007.00391.x>
- 794 Haralick, R.M., Shanmugam, K., Dinstein, I., 1973. Textural Features for Image Classification. *IEEE*
795 *Trans. Syst. Man Cybern.* SMC-3, 610–621. <https://doi.org/10.1109/TSMC.1973.4309314>
- 796 Hebbar, R., Ravishankar, H.M., Trivedi, S., Manjula, V.B., Kumar, N.M., Mukharib, D.S., Mote, J.K.,
797 Sudeesh, S., Raj, U., Raghuramulu, Y., Ganesh Raj, K., 2019. National Level Inventory of
798 Coffee Plantations using High-Resolution Satellite Data. *ISPRS - Int. Arch. Photogramm.*
799 *Remote Sens. Spat. Inf. Sci.* XLII-3/W6, 293–298. [https://doi.org/10.5194/isprs-archives-XLII-](https://doi.org/10.5194/isprs-archives-XLII-3-W6-293-2019)
800 [3-W6-293-2019](https://doi.org/10.5194/isprs-archives-XLII-3-W6-293-2019)
- 801 Hengl, T., Nussbaum, M., Wright, M.N., Heuvelink, G.B.M., Gräler, B., 2018. Random forest as a
802 generic framework for predictive modeling of spatial and spatio-temporal variables. *PeerJ* 6,
803 e5518. <https://doi.org/10.7717/peerj.5518>
- 804 Housman, I., Chastain, R., Finco, M., 2018. An Evaluation of Forest Health Insect and Disease Survey
805 Data and Satellite-Based Remote Sensing Forest Change Detection Methods: Case Studies
806 in the United States. *Remote Sens.* 10, 1184. <https://doi.org/10.3390/rs10081184>
- 807 Hu, L., Li, W., Xu, B., 2018. Monitoring mangrove forest change in China from 1990 to 2015 using
808 Landsat-derived spectral-temporal variability metrics. *Int. J. Appl. Earth Obs. Geoinformation*
809 73, 88–98. <https://doi.org/10.1016/j.jag.2018.04.001>
- 810 Hung Anh, N., Bokelmann, W., Thi Nga, D., Van Minh, N., 2019. Toward Sustainability or Efficiency:
811 The Case of Smallholder Coffee Farmers in Vietnam. *Economies* 7, 66.
812 <https://doi.org/10.3390/economies7030066>
- 813 Hunt, D.A., Tabor, K., Hewson, J.H., Wood, M.A., Reymondin, L., Koenig, K., Schmitt-Harsh, M.,
814 Follett, F., 2020. Review of Remote Sensing Methods to Map Coffee Production Systems.
815 *Remote Sens.* 12, 2041. <https://doi.org/10.3390/rs12122041>
- 816 Hurni, K., Fox, J., 2018. The expansion of tree-based boom crops in mainland Southeast Asia: 2001 to
817 2014. *J. Land Use Sci.* 13, 198–219. <https://doi.org/10.1080/1747423X.2018.1499830>
- 818 Inglada, J., Arias, M., Tardy, B., Hagolle, O., Valero, S., Morin, D., Dedieu, G., Sepulcre, G.,
819 Bontemps, S., Defourny, P., Koetz, B., 2015. Assessment of an Operational System for Crop
820 Type Map Production Using High Temporal and Spatial Resolution Satellite Optical Imagery.
821 *Remote Sens.* 7, 12356–12379. <https://doi.org/10.3390/rs70912356>
- 822 Jain, M., Mondal, P., DeFries, R.S., Small, C., Galford, G.L., 2013. Mapping cropping intensity of
823 smallholder farms: A comparison of methods using multiple sensors. *Remote Sens. Environ.*
824 134, 210–223. <https://doi.org/10.1016/j.rse.2013.02.029>

- 825 Jezeer, R.E., Santos, M.J., Verweij, P.A., Boot, R.G.A., Clough, Y., 2019. Benefits for multiple
826 ecosystem services in Peruvian coffee agroforestry systems without reducing yield. *Ecosyst.*
827 *Serv.* 40, 101033. <https://doi.org/10.1016/j.ecoser.2019.101033>
- 828 Jin, Z., Azzari, G., You, C., Di Tommaso, S., Aston, S., Burke, M., Lobell, D.B., 2019. Smallholder
829 maize area and yield mapping at national scales with Google Earth Engine. *Remote Sens.*
830 *Environ.* 228, 115–128. <https://doi.org/10.1016/j.rse.2019.04.016>
- 831 Kath, J., Byrareddy, V.M., Craparo, A., Nguyen-Huy, T., Mushtaq, S., Cao, L., Bossolasco, L., 2020.
832 Not so robust: Robusta coffee production is highly sensitive to temperature. *Glob. Change*
833 *Biol.* 26, 3677–3688. <https://doi.org/10.1111/gcb.15097>
- 834 Kawakubo, F.S., Pérez Machado, R.P., 2016. Mapping coffee crops in southeastern Brazil using
835 spectral mixture analysis and data mining classification. *Int. J. Remote Sens.* 37, 3414–3436.
836 <https://doi.org/10.1080/01431161.2016.1201226>
- 837 Kelley, L.C., Pitcher, L., Bacon, C., 2018. Using Google Earth Engine to Map Complex Shade-Grown
838 Coffee Landscapes in Northern Nicaragua. *Remote Sens.* 10, 952.
839 <https://doi.org/10.3390/rs10060952>
- 840 Läderach, P., Ramirez-Villegas, J., Navarro-Racines, C., Zelaya, C., Martinez-Valle, A., Jarvis, A.,
841 2017. Climate change adaptation of coffee production in space and time. *Clim. Change* 141,
842 47–62. <https://doi.org/10.1007/s10584-016-1788-9>
- 843 Leakey, R.R.B., 2017. Agroforestry Tree Products (AFTPs): Targeting Poverty Reduction and
844 Enhanced Livelihoods, in: *Multifunctional Agriculture*. Elsevier, pp. 123–138.
845 <https://doi.org/10.1016/B978-0-12-805356-0.00013-1>
- 846 Liu, P., Chen, X., 2019. Intercropping Classification From GF-1 and GF-2 Satellite Imagery Using a
847 Rotation Forest Based on an SVM. *ISPRS Int. J. Geo-Inf.* 8, 86.
848 <https://doi.org/10.3390/ijgi8020086>
- 849 Mercier, A., Betbeder, J., Rumiano, F., Baudry, J., Gond, V., Blanc, L., Bourgoin, C., Cornu, G.,
850 Ciudad, C., Marchamalo, M., Pocard-Chapuis, R., Hubert-Moy, L., 2019. Evaluation of
851 Sentinel-1 and 2 Time Series for Land Cover Classification of Forest–Agriculture Mosaics in
852 Temperate and Tropical Landscapes. *Remote Sens.* 11, 979.
853 <https://doi.org/10.3390/rs11080979>
- 854 Meyfroidt, P., Vu, T.P., Hoang, V.A., 2013. Trajectories of deforestation, coffee expansion and
855 displacement of shifting cultivation in the Central Highlands of Vietnam. *Glob. Environ.*
856 *Change* 23, 1187–1198. <https://doi.org/10.1016/j.gloenvcha.2013.04.005>
- 857 Mishra, V.N., Prasad, R., Rai, P.K., Vishwakarma, A.K., Arora, A., 2019. Performance evaluation of
858 textural features in improving land use/land cover classification accuracy of heterogeneous
859 landscape using multi-sensor remote sensing data. *Earth Sci. Inform.* 12, 71–86.
860 <https://doi.org/10.1007/s12145-018-0369-z>
- 861 Monfreda, C., Ramankutty, N., Foley, J.A., 2008. Farming the planet: 2. Geographic distribution of
862 crop areas, yields, physiological types, and net primary production in the year 2000: GLOBAL
863 CROP AREAS AND YIELDS IN 2000. *Glob. Biogeochem. Cycles* 22, n/a-n/a.
864 <https://doi.org/10.1029/2007GB002947>
- 865 Mukashema, A., Veldkamp, A., Vrieling, A., 2014. Automated high resolution mapping of coffee in
866 Rwanda using an expert Bayesian network. *Int. J. Appl. Earth Obs. Geoinformation* 33, 331–
867 340. <https://doi.org/10.1016/j.jag.2014.05.005>
- 868 Müller, D., Zeller, M., 2002. Land use dynamics in the central highlands of Vietnam: a spatial model
869 combining village survey data with satellite imagery interpretation. *Agric. Econ.* 23.

- 870 Müller, H., Rufin, P., Griffiths, P., Barros Siqueira, A.J., Hostert, P., 2015. Mining dense Landsat time
871 series for separating cropland and pasture in a heterogeneous Brazilian savanna landscape.
872 *Remote Sens. Environ.* 156, 490–499. <https://doi.org/10.1016/j.rse.2014.10.014>
- 873 Nesper, M., Kueffer, C., Krishnan, S., Kushalappa, C.G., Ghazoul, J., 2017. Shade tree diversity
874 enhances coffee production and quality in agroforestry systems in the Western Ghats. *Agric.
875 Ecosyst. Environ.* 247, 172–181. <https://doi.org/10.1016/j.agee.2017.06.024>
- 876 Nguyen, M.D., Villanueva, O.B., Bui, D.D., Nguyen, P.T., Ribbe, L., 2019. Harmonization of Landsat
877 and Sentinel 2 for Crop Monitoring in Drought Prone Areas: Case Studies of Ninh Thuan
878 (Vietnam) and Bekaa (Lebanon). *Remote Sens.*
879 <https://doi.org/10.20944/preprints201910.0275.v1>
- 880 Nogueira, S.M.C., Moreira, M.A., Volpato, M.M.L., 2018. Relationship between coffee crop productivity
881 and vegetation indexes derived from OLI / Landsat-8 Sensor Data with and without
882 topographic correction. *Eng. Agric.* 38, 387–394. [https://doi.org/10.1590/1809-4430-](https://doi.org/10.1590/1809-4430-eng.agric.v38n3p387-394/2018)
883 [eng.agric.v38n3p387-394/2018](https://doi.org/10.1590/1809-4430-eng.agric.v38n3p387-394/2018)
- 884 Nomura, K., Mitchard, E., 2018. More Than Meets the Eye: Using Sentinel-2 to Map Small Plantations
885 in Complex Forest Landscapes. *Remote Sens.* 10, 1693. <https://doi.org/10.3390/rs10111693>
- 886 Numbisi, F.N., Van Coillie, F.M.B., De Wulf, R., 2019. Delineation of Cocoa Agroforests Using Multi-
887 Season Sentinel-1 SAR Images: Low Grey Level Range Reduces Uncertainties in GLCM
888 Texture-Based Mapping. *Int. J. Geo-Inf.* <https://doi.org/10.20944/preprints201901.0050.v1>
- 889 O'Brien, R.M., 2007. A Caution Regarding Rules of Thumb for Variance Inflation Factors 18.
- 890 Oon, A., Ngo, K.D., Azhar, R., Ashton-Butt, A., Lechner, A.M., Azhar, B., 2019. Assessment of ALOS-
891 2 PALSAR-2L-band and Sentinel-1 C-band SAR backscatter for discriminating between large-
892 scale oil palm plantations and smallholdings on tropical peatlands. *Remote Sens. Appl. Soc.
893 Environ.* 13, 183–190. <https://doi.org/10.1016/j.rsase.2018.11.002>
- 894 Ortega-Huerta, M.A., Komar, O., Price, K.P., Ventura, H.J., 2012. Mapping coffee plantations with
895 Landsat imagery: an example from El Salvador. *Int. J. Remote Sens.* 33, 220–242.
896 <https://doi.org/10.1080/01431161.2011.591442>
- 897 Padovan, M.P., Brook, R.M., Barrios, M., Cruz-Castillo, J.B., Vilchez-Mendoza, S.J., Costa, A.N.,
898 Rapidel, B., 2018. Water loss by transpiration and soil evaporation in coffee shaded by
899 *Tabebuia rosea* Bertol. and *Simarouba glauca* dc. compared to unshaded coffee in sub-
900 optimal environmental conditions. *Agric. For. Meteorol.* 248, 1–14.
901 <https://doi.org/10.1016/j.agrformet.2017.08.036>
- 902 Pflugmacher, D., Rabe, A., Peters, M., Hostert, P., 2019. Mapping pan-European land cover using
903 Landsat spectral-temporal metrics and the European LUCAS survey. *Remote Sens. Environ.*
904 221, 583–595. <https://doi.org/10.1016/j.rse.2018.12.001>
- 905 Pham, Y., Reardon-Smith, K., Mushtaq, S., Cockfield, G., 2019. The impact of climate change and
906 variability on coffee production: a systematic review. *Clim. Change* 156, 609–630.
907 <https://doi.org/10.1007/s10584-019-02538-y>
- 908 Pham, Y., Reardon-Smith, K., Mushtaq, S., Deo, R.C., 2020. Feedback modelling of the impacts of
909 drought: A case study in coffee production systems in Viet Nam. *Clim. Risk Manag.* 30,
910 100255. <https://doi.org/10.1016/j.crm.2020.100255>
- 911 Pham-Thanh, H., Linden, R., Ngo-Duc, T., Nguyen-Dang, Q., Fink, A.H., Phan-Van, T., 2020.
912 Predictability of the rainy season onset date in Central Highlands of Vietnam. *Int. J. Climatol.*
913 40, 3072–3086. <https://doi.org/10.1002/joc.6383>
- 914 Phuc, X., Tran, H.N., 2014. Rubber Expansion and Forest Protection in Vietnam.

- 915 Pontius, R.G., Millones, M., 2011. Death to Kappa: birth of quantity disagreement and allocation
916 disagreement for accuracy assessment. *Int. J. Remote Sens.* 32, 4407–4429.
917 <https://doi.org/10.1080/01431161.2011.552923>
- 918 Poortinga, A., Tenneson, K., Shapiro, A., Nquyen, Q., San Aung, K., Chishtie, F., Saah, D., 2019.
919 Mapping Plantations in Myanmar by Fusing Landsat-8, Sentinel-2 and Sentinel-1 Data along
920 with Systematic Error Quantification. *Remote Sens.* 11, 831.
921 <https://doi.org/10.3390/rs11070831>
- 922 Qadir, A., Mondal, P., 2020. Synergistic Use of Radar and Optical Satellite Data for Improved
923 Monsoon Cropland Mapping in India. *Remote Sens.* 12, 522.
924 <https://doi.org/10.3390/rs12030522>
- 925 Schmitt, M., Hughes, L.H., Qiu, C., Zhu, X.X., 2019. Aggregating cloud-free sentinel-2 images with
926 google earth engine. *ISPRS Ann. Photogramm. Remote Sens. Spat. Inf. Sci.* IV-2/W7, 145–
927 152. <https://doi.org/10.5194/isprs-annals-IV-2-W7-145-2019>
- 928 Scornet, E., 2017. Tuning parameters in random forests. *ESAIM Proc. Surv.* 60, 144–162.
929 <https://doi.org/10.1051/proc/201760144>
- 930 See, L., Fritz, S., You, L., Ramankutty, N., Herrero, M., Justice, C., Becker-Reshef, I., Thornton, P.,
931 Erb, K., Gong, P., Tang, H., van der Velde, M., Ericksen, P., McCallum, I., Kraxner, F.,
932 Obersteiner, M., 2015. Improved global cropland data as an essential ingredient for food
933 security. *Glob. Food Secur.* 4, 37–45. <https://doi.org/10.1016/j.gfs.2014.10.004>
- 934 Siebert, S.F., 2002. From shade- to sun-grown perennial crops in Sulawesi, Indonesia: implications for
935 biodiversity conservation and soil fertility. *Biodivers. Conserv.* 14.
- 936 Spracklen, B., Spracklen, D.V., 2021. Synergistic Use of Sentinel-1 and Sentinel-2 to Map Natural
937 Forest and Acacia Plantation and Stand Ages in North-Central Vietnam. *Remote Sens.* 13,
938 185. <https://doi.org/10.3390/rs13020185>
- 939 Sun, C., Bian, Y., Zhou, T., Pan, J., 2019. Using of Multi-Source and Multi-Temporal Remote Sensing
940 Data Improves Crop-Type Mapping in the Subtropical Agriculture Region. *Sensors* 19, 2401.
941 <https://doi.org/10.3390/s19102401>
- 942 Thi, T.P., Chaovanapoonphol, Y., 2014. An Evaluation of Adaptation Options to Climate Pressure on
943 Highland Robusta Coffee Production, Daklak Province, Vietnam. *World J. Agric. Res.* 2, 205–
944 215. <https://doi.org/10.12691/wjar-2-5-2>
- 945 Torbick, N., Ledoux, L., Salas, W., Zhao, M., 2016. Regional Mapping of Plantation Extent Using
946 Multisensor Imagery. *Remote Sens.* 8, 236. <https://doi.org/10.3390/rs8030236>
- 947 Tsai, D.-M., Chen, W.-L., 2017. Coffee plantation area recognition in satellite images using Fourier
948 transform. *Comput. Electron. Agric.* 135, 115–127.
949 <https://doi.org/10.1016/j.compag.2016.12.020>
- 950 Waldner, F., Chen, Y., Lawes, R., Hochman, Z., 2019. Needle in a haystack: Mapping rare and
951 infrequent crops using satellite imagery and data balancing methods. *Remote Sens. Environ.*
952 233, 111375. <https://doi.org/10.1016/j.rse.2019.111375>
- 953 Widayati, A., Verbist, B., Meijerink, A., 2003. Application of combined pixel-based and spatial-based
954 approaches for improved mixed vegetation classification using Ikonos.
- 955
- 956

957 List of Figure Captions

958 *Figure 1.* A) The Central Highlands region, Dak Lak province, and Ea H'Leo district; B)
959 Elevation in Dak Lak (Farr et al., 2007) and C) Land cover map of Dak Lak, MODIS-derived
960 Land cover product (Friedl & Sulla-Menashe, 2015).

961 *Figure 2.* Methods workflow showing data used, pre-processing steps and classification
962 inputs and outputs.

963 *Figure 3.* Map of detailed land cover classification for Dak Lak, at 10-m resolution.

964 *Figure 4.* Closer look at the detailed land cover map in order to highlight specific landscape
965 processes being captured, along with the corresponding satellite images: A) concentration of
966 many new coffee plots, in a sun coffee and rubber landscape in Ea H'Leo, B) establishment
967 of newly planted coffee in M'Drak (Eastern-most district), C) area dominated by sun coffee in
968 Krong Ana, D) high concentration of intercropped or shade coffee near Buon Ma Thuot, E)
969 zoomed in view near Buon Ma Thuot, an area of mixed sun and intercropped plots.

970 *Figure 5.* Comparison of A) the binary coffee map from this study; B) the orchard class from
971 the 2017 JAXA Land cover map (10m), derived from S2, Landsat 7 & 8, ALOS/AVNIR-2,
972 PALSAR, and SRTM (Duong et. al., 2018); C) Humi and Fox's (2018) coffee class from their
973 2014 boom crop mapping in Mainland Southeast Asia (250m), MODIS-derived; D) Monfreda
974 et al., (2008) "fraction of harvested area," with a threshold of more than 1% coffee area
975 harvested, disaggregated at the 5' (~10km) grid cell from agricultural statistics for 2000.

976